Cell Metabolism
Article

The Glucagon Receptor Is Required for the Adaptive Metabolic Response to Fasting

Christine Longuet,[1] Elaine M. Sinclair,[1] Adriano Maida,[1] Laurie L. Baggio,[1] Marlena Maziarz,[1] Maureen J. Charron,[2] and Daniel J. Drucker[1,*]
[1]Department of Medicine, Samuel Lunenfeld Research Institute, Mount Sinai Hospital, University of Toronto, Toronto, Ontario M5G 1X5, Canada
[2]Department of Biochemistry, Albert Einstein College of Medicine, Bronx, NY 10461, USA
*Correspondence: d.drucker@utoronto.ca
DOI 10.1016/j.cmet.2008.09.008

SUMMARY

Glucagon receptor (Gcgr) signaling maintains hepatic glucose production during the fasting state; however, the importance of the Gcgr for lipid metabolism is unclear. We show here that fasted Gcgr−/− mice exhibit a significant increase in hepatic triglyceride secretion and fasting increases fatty acid oxidation (FAO) in wild-type (WT) but not in Gcgr−/− mice. Moreover fasting upregulated the expression of FAO-related hepatic mRNA transcripts in Gcgr+/+ but not in Gcgr−/− mice. Exogenous glucagon administration reduced plasma triglycerides in WT mice, inhibited TG synthesis and secretion, and stimulated FA beta oxidation in Gcgr+/+ hepatocytes. The actions of glucagon on TG synthesis and FAO were abolished in PPARα−/− hepatocytes. These findings demonstrate that the Gcgr receptor is required for control of lipid metabolism during the adaptive metabolic response to fasting.

INTRODUCTION

Glucagon, a peptide of 29 amino acids released from pancreatic α cells is the principal counterregulatory hormone that opposes the actions of insulin. Glucagon stimulates gluconeogenesis and promotes glycogenolysis leading to liberation of glucose from hepatocytes. These actions of glucagon are transduced via a G protein-coupled receptor (GPCR) (the glucagon receptor or Gcgr), a member of the class II GPCR superfamily (Mayo et al., 2003). Glucagon action in the liver maintains normoglycemia in the fasted state via activation of a Gs protein, leading to the stimulation of adenylate cyclase activity, cAMP production, Epac, Torc2, PKA, and CREB activation (Jelinek et al., 1993; Koo et al., 2005; Wakelam et al., 1986). Glucagon also increases intracellular calcium in a phospholipase C dependent manner (Aromataris et al., 2006; Jelinek et al., 1993; Wakelam et al., 1986) and activates AMPK (Kimball et al., 2004) p38 MAPK (Cao et al., 2005; Chen et al., 1998) and JNK (Chen et al., 1998), through mechanisms that remain incompletely understood.

The control of glucagon secretion is dysregulated in human subjects with type 2 diabetes (T2DM) (Raskin and Unger, 1978; Unger, 1971), fostering efforts directed at suppression of glucagon action for the treatment of T2DM. Indeed, diminution of glucagon action leads to reductions in blood glucose and improvement in glucose control in preclinical studies (Jiang and Zhang, 2003; Johnson et al., 1982; Unson et al., 1989). Moreover, transient reduction of hepatic Gcgr expression in diabetic rodents was associated with significant improvements in glucose control (Liang et al., 2004; Sloop et al., 2004), and genetic inactivation of the Gcgr in mice is associated with mild fasting hypoglycemia, improved glucose tolerance, and resistance to diet-induced obesity (Conarello et al., 2007; Gelling et al., 2003). Taken together, these studies confirm the importance of Gcgr signaling in the control of glucose homeostasis.

Improvement of metabolic control in the setting of glucose intolerance or experimental diabetes through attenuation of glucagon action has been associated with reduction in hepatic lipid accumulation and reduced levels of circulating triglycerides and free fatty acids (Conarello et al., 2007; Liang et al., 2004). Nevertheless, glucagon administration in the absence of diabetes produces potent hypolipemic actions (Bobe et al., 2003a; Eaton, 1973; Guettet et al., 1991) including decreased triglyceride (TG) and very low density lipoproteins (VLDL) release by the liver (Bobe et al., 2003a; Guettet et al., 1989), reduced levels of plasma cholesterol (Guettet et al., 1988, 1989) and stimulation of hepatic free fatty acid (FFA) beta oxidation (Prip-Buus et al., 1990). Indeed, exogenous glucagon reduces liver triacylglycerol content and prevents the development of fatty liver in dairy cows (Bobe et al., 2003b, 2006; Nafikov et al., 2006), whereas reduced glucagon action is associated with the development of fatty liver (Charbonneau et al., 2005a, 2005b).

As the mechanisms linking Gcgr action to the control of lipid synthesis and/or FFA oxidation are poorly understood, we have now examined the importance of Gcgr signaling for lipid synthesis, secretion, and oxidation in Gcgr+/+ and Gcgr−/− mice. Our data provide new evidence implicating the Gcgr as an important integrator of metabolic signals converging on the peroxisome proliferator-activated receptor (PPARα), leading to regulation of multiple components of hepatocyte lipid metabolism.

RESULTS

The Gcgr Is Required for Control of Hepatic TG Secretion

To assess the importance of Gcgr signaling for the regulation of plasma lipids, we measured circulating levels of TGs and FFA in Gcgr−/− and Gcgr+/+ littermate control mice after fasting. No

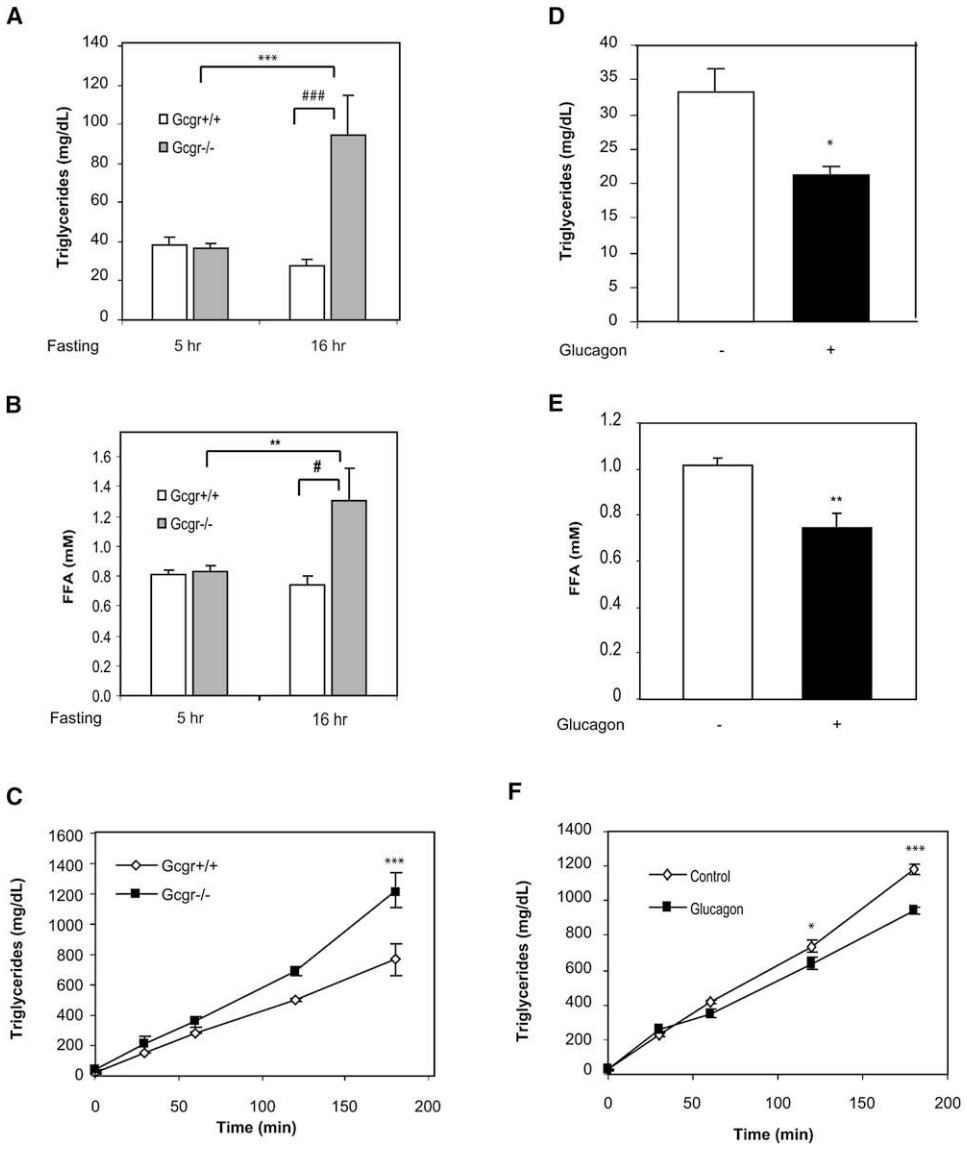

Figure 1. Glucagon Decreases Levels of Plasma TGs and Inhibits Hepatic TG Secretion In Vivo

(A–F) TG (A and D) and FFA (B and E) levels were determined in plasma from Gcgr−/− male mice, and Gcgr+/+ littermate controls fasted for 5 or 16 hr (A and B) or from WT males treated with glucagon for 24 hr (30 ng/g body weight) as described in the Experimental Procedures (D and E). In (C) and (F), hepatic TG secretion was assessed indirectly by measurement of plasma TGs after intravenous injection of Triton WR-1339 in Gcgr−/− mice and +/+ littermate controls fasted for 16 hr (C), or WT males following a single glucagon injection, 30 ng/g BW as described in the Experimental Procedures (F). Values in each panel are expressed as mean ± SEM n = 4–11 mice per group. * = $p < 0.05$; ** or # = $p < 0.01$; *** = $p < 0.001$. ### = $p < 0.001$.

difference was observed in levels of plasma TGs and FFA in male Gcgr−/− versus Gcgr+/+ mice after 5 hr of fasting (Figures 1A and 1B), and TG levels were further reduced by 28% in Gcgr+/+ mice after 16 hr of fasting (Figure 1A). Unexpectedly, Gcgr−/− mice exhibited a marked increase in plasma TGs and FFA after a 16 hr fast (Figures 1A and 1B, $p < 0.001$; and Figures S1A and S1B). Hepatic TG secretion, assessed following administration of triton WR1339 (Otway and Robinson, 1967; Scanu, 1965), was also significantly increased in male (Figure 1C, $p < 0.001$) and female Gcgr−/− mice (Figure S1C). Consistent with findings in Gcgr−/− mice, exogenous glucagon administration significantly decreased levels of plasma TGs and FFA in both male (Figures 1D and 1E) and female (Figures S1D and S1E) Gcgr+/+ mice. Similarly, glucagon inhibited hepatic TG secretion by 20% in male (Figure 1F, $p < 0.001$) and 30% in female (Figure S1F) Gcgr+/+ mice.

The effects of glucagon on plasma lipids were not secondary to stimulation of insulin secretion, as levels of plasma insulin level and glucose were appropriately lower after fasting in both Gcgr+/+ and Gcgr−/− mice (Figures S2A and S2B), and glucagon administration significantly increased glycemia (Figure S2D) but produced only modest increases in levels of plasma insulin (Figure S2C). Moreover, unlike the effects of exogenous glucagon (Figure 1F), which reduced TG secretion, insulin

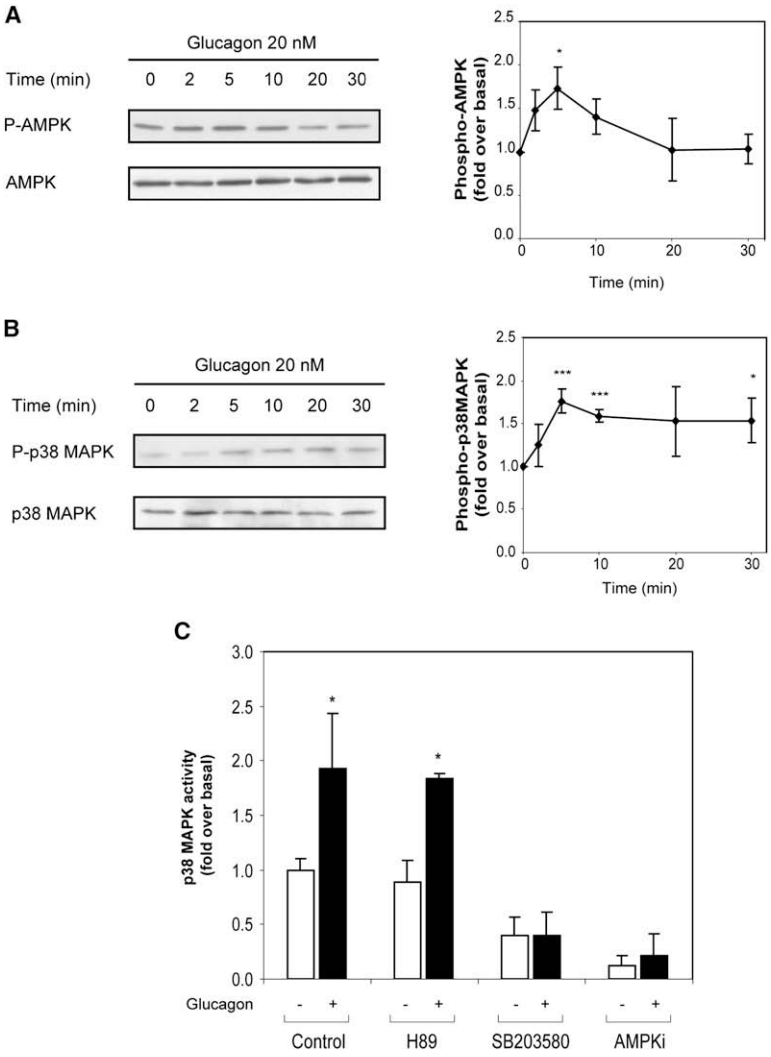

Figure 2. Glucagon Activates p38 MAPK in an AMPK-Dependent Manner

(A and B) Primary mouse hepatocytes from WT mice were cultured with or without 20 nM glucagon, following which total cell lysates were prepared and subjected to western blot analysis as described in the Experimental Procedures. * = $p < 0.05$, *** = $p < 0.001$ for levels of phosphorylated proteins in the presence or absence of glucagon.

(C) Mouse hepatocytes were cultured for 30 min with or without 20 nM glucagon in the presence or absence of 2 μM H89, 10 μM SB203580, or 20 μM AMPKi. All data are mean ± SEM, n = 6. * = $p < 0.01$ for values obtained in the presence or absence of glucagon.

administration reduced glycemia (Figure S2F) but did not reduce TG secretion (Figure S2E). Similarly, while glucagon directly inhibited both TG synthesis and secretion in murine hepatocytes in vitro, insulin exerted opposite stimulatory effects (Figures S2G and S2H). Therefore, the inhibitory effects of glucagon on TG synthesis and secretion are not likely mediated through stimulation of insulin secretion.

To elucidate the mechanisms important for glucagon action on lipid metabolism, we analyzed p38 MAPK and AMPK, signaling molecules known to be important for the regulation of hepatic lipid metabolism. Glucagon rapidly and transiently stimulated both AMPK and p38 MAPK phosphorylation in murine hepatocytes (Figures 2A and 2B, respectively). Moreover, glucagon stimulated p38 MAPK activity and the p38 MAPK inhibitor SB203580 and the AMPK inhibitor (AMPKi) (but not the PKA inhibitor H89) prevented the glucagon-stimulated increase in p38 MAPK activity (Figure 2C).

Glucagon Inhibits TG Synthesis and Secretion via Distinct Pathways

We next investigated the glucagon-regulated control of hepatocyte TG synthesis and secretion in murine hepatocytes. Glucagon had no effect on the intracellular levels of newly synthesized FFA in hepatocytes (Figure 3A), but significantly inhibited both TG synthesis (Figure 3B, $p < 0.001$) and secretion (Figure 3C, $p < 0.001$). The inhibitory actions of glucagon on both TG synthesis and secretion were not diminished by the PKA inhibitor H89 (Figures 3B and 3C, respectively). In contrast, the glucagon-mediated inhibition of TG synthesis (Figure 3B), but not secretion (Figure 3C), was abolished following pharmacological inhibition of either p38 MAPK or AMPK. Similarly, glucagon was not able to inhibit TG synthesis but still inhibited TG secretion (Figures S3B and S3C) following shRNA-mediated knockdown (by about 50%, Figure S3A) of p38MAPK and AMPK expression in hepatocytes.

FFA beta oxidation in liver homogenates from fasted and fed mice was monitored as conversion of 1-^{14}C palmitate to $^{14}CO_2$, which increases linearly in hepatocytes as the rate of beta oxidation increases (Giordano et al., 2005). Fasting increased hepatic FFA oxidation in Gcgr+/+ mice (Figure 3D, 1.25 ± 0.05 μmol/g liver/hr in fed versus 1.84 ± 0.1 μmol/g liver/hr in fasted mice, $p < 0.01$). In contrast, FFA oxidation failed to increase and paradoxically decreased in fasting Gcgr−/− mice (Figure 3D, 1.84 ± 0.1 μmol/g liver/hr versus 0.53 ± 0.08 μmol/g liver/hr in fasted Gcgr+/+ versus Gcgr−/− mice, respectively, $p < 0.001$). Moreover, FFA oxidation was also significantly lower in fed Gcgr−/− mice (Figure 3D; $p < 0.05$, 1.25 ± 0.05 μmol/g liver/hr in Gcgr+/+ versus 0.92 ± 0.04 μmol/g liver/hr in Gcgr−/− mice, $p < 0.01$). The glucagon-stimulated increase in FFA beta oxidation was completely abolished by the p38 MAPK inhibitor SB203580 (Figure 3E), and no beta oxidation of fatty acids was detectable under basal or glucagon-stimulated conditions when hepatocytes were pretreated with AMPKi (Figure 3E). Reduction of p38MAPK and AMPK expression using shRNA also abrogated the glucagons-stimulated increase in FAO oxidation (Figure S3D).

To determine whether the inhibitory effect of glucagon on TG synthesis may be indirect, perhaps reflecting reduced availability of FFA due to enhanced glucagon-stimulated fatty acid oxidation, we examined whether inhibition of fatty acid oxidation results in increased levels of FFA available for TG synthesis. Hepatocytes were incubated with 1 μM etomoxir, an irreversible

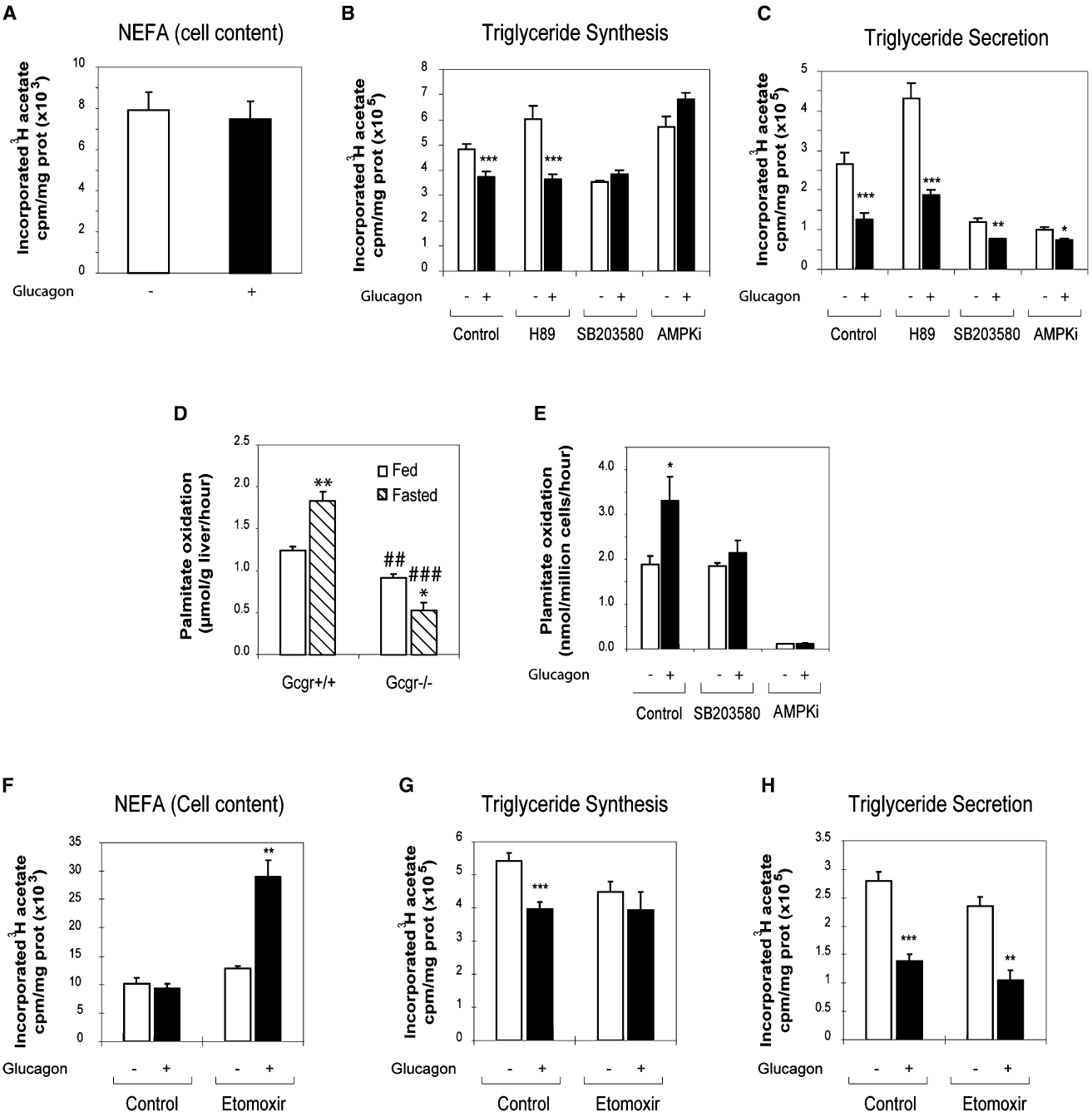

Figure 3. Glucagon Modulates Hepatic TG Synthesis and Secretion and FFA Beta Oxidation

(A–H)Lipid synthesis was assessed by measurement of FFAs and TGs in WT hepatocytes (A, B, C, F, G, and H) treated for 16 hr with or without 20 nM glucagon in the presence or absence of 10 μM SB203580, 2 μM H89, or 20 μM AMPKi (A–C) or 1 μM etomoxir (F–H). Lipids were extracted from the media (secretion) or cells + media (synthesis), separated by TLC, and quantified by scintillation counting. Data are mean ± SEM of four independent experiments. * = $p < 0.05$, ** = $p < 0.01$, *** = $p < 0.001$ for values obtained in the presence or absence of glucagon. Beta oxidation of [1-^{14}C]-palmitate assessed in liver homogenates were prepared from Gcgr−/− or littermate controls fed or fasted for 24 hr (D),a nd in primary hepatocytes from WT mice treated with or without 20 nM glucagon for 24 hr in the presence or absence of 10 μM SB203580 or 20 μM AMPKi (E), as described in the Experimental Procedures. Data are mean ± SEM of six independent experiments. * = $p < 0.05$, ** = $p < 0.01$ for fasted versus the fed state in (D) and for vehicle versus glucagon treated cells in (E); ## = $p < 0.01$, ### = $p < .001$ for Gcgr+/+ versus Gcgr−/− mice in (D).

CPT1a antagonist known to inhibit FAO (Hiyoshi et al., 2003). Although glucagon alone had no significant effect on levels of FFAs in murine hepatocytes, glucagon stimulated a significant increase in levels of FFAs in hepatocytes treated with etomoxir (Figure 3F). Moreover, glucagon no longer inhibited TG synthesis but continued to inhibit TG secretion in the presence of etomoxir

(Figures 3G and 3H). We conclude that glucagon inhibits TG synthesis by increasing FFA beta oxidation, thereby decreasing the availability of FFA for TG secretion.

To understand the mechanism(s) by which glucagon modulates the adaptation of hepatic lipid metabolism to fasting, we analyzed hepatic gene expression profiles in fasted Gcgr+/+ versus Gcgr−/− mice. Fasting increased levels of mRNA transcripts for multiple genes important for control of fatty acid beta oxidation in male and female Gcgr+/+ mice (Figures 4A and S4A). In contrast, levels of several mRNA transcripts of genes important for FAO were modestly increased in Gcgr−/− mice (compare Figures 4A and 4B), and more prolonged fasting in Gcgr−/− mice failed to upregulate levels of hepatic mRNA transcripts for Facl2, Derc2, CPT2, Acadm, Ehadh, Hadha, Hadhb (Figures 4B and S4B). Consistent with the importance of glucagon for changes in hepatic gene expression during fasting, exogenous administration of glucagon to WT mice produced a hepatic gene expression profile comparable to that detected during fasting, with significant increases in levels of mRNA transcripts for multiple genes involved in fatty acid beta oxidation (Figures 4C and S4C).

In contrast to the importance of the Gcgr for fasting-related changes in genes regulating FAO, the expression of genes regulating fatty acid synthesis was similarly decreased in Gcgr+/+ and Gcgr−/− mice during fasting (Figures 4D, 4E, S4D, and S4E). Furthermore, exogenous glucagon administration did not produce a reduction in levels of mRNA transcripts for the majority of genes regulating fatty acid synthesis (Figures 4F and S4F). These findings demonstrate that the Gcgr is essential for control of a genetic program regulating fatty acid beta oxidation; however, Gcgr signaling is not essential for control of genes regulating fatty acid synthesis.

Glucagon Stimulates PPARα Activity in a p38 MAPK- and AMPK-Dependent Manner

As many of the glucagon-regulated genes important for fatty acid β oxidation (Figures 4 and S4) are known targets of PPARα (Patsouris et al., 2006), we assessed the role of PPARα as a downstream target for glucagon action. Levels of liver PPARα mRNA transcripts were comparable in fasted Gcgr−/− versus Gcgr+/+ mice (Figure 5A), and exogenous glucagon produced a modest but nonsignificant increase in levels of PPARα mRNA transcripts in WT mice (Figure 5B). Furthermore, hepatic PPARα protein levels increased to similar levels during fasting in both Gcgr+/+ and Gcgr−/− mice (Figure 5C). However, glucagon administration was associated with a marked redistribution in PPARα immunoreactivity from the cytoplasm to hepatocyte nuclei (Figure 5D, lower panel). Furthermore, fasting was associated with nuclear translocation of PPARα in liver of Gcgr+/+ mice, but not in Gcgr−/− mice, in which considerable amounts of PPARα remained in the cytoplasm (Figure 5E). Moreover, fasting increased the binding of PPARα to a peroxisome proliferator response element (PPRE) in EMSA studies using liver nuclear extracts from Gcgr+/+ mice but not in extracts from fasted Gcgr−/− mice (Figure 5F).

To understand the mechanisms by which PPARα remains in the cytoplasm under the fed state, we investigated the interaction of PPARα with the chaperone protein HSP90. Under resting conditions PPARα is bound to HSP90 in the cytoplasm and upon activation, dissociates from HSP90, and translocates to the nucleus to activate the transcription of target genes (Sumanasekera et al., 2003a, 2003b). Consistent with a role for HSP90 in the regulation of PPARα activity, the HSP90 inhibitor 17DMAG significantly enhanced glucagon-induced PPARα activity (Figure 6A). Furthermore, we observed a physical interaction of PPARα with HSP90 in the cytoplasmic fraction prepared from primary murine hepatocyte cultures (Figure 6B). Moreover, the ability of glucagon to reduce the cytoplasmic localization and enhance the nuclear expression of phosphorylated PPARα was markedly enhanced in the presence of 17DMAG (Figure 6B). Taken together, these data suggest that HSP90 is a chaperone for PPARα in hepatocyte cytoplasm, and the HSP90-PPARα interaction may regulate the extent of glucagon-dependent PPARα activation in the nucleus.

To assess whether the nuclear translocation of PPARα was associated with an increase in PPARα-dependent transcriptional activity, hepatocytes were transfected with a luciferase reporter gene containing three tandem copies of a PPRE. Glucagon increased PPRE-dependent luciferase activity by more than 4.5-fold in WT hepatocytes (Figure 6C, $p < 0.01$). As the PPRE integrates transcriptional responses from PPARα, PPARβ, and PPARγ, we verified the importance of PPARα as a downstream target of glucagon action using PPARα knockout (PPARα−/−) mice. Indeed, the glucagon-stimulated induction of PPRE-dependent luciferase activity was substantially diminished in PPARα−/− versus +/+ hepatocytes (Figure 6C, $p < 0.01$). Hence, more than 70% of the glucagon-stimulated induction of PPRE transcriptional activity in hepatocytes is mediated by PPARα. This increase in PPARα activity upon glucagon stimulation was lost in Gcgr−/− hepatocytes (Figure S5A). Furthermore, glucagon's effect on PPARα activation in Gcgr+/+ hepatocytes was similar and nonadditive to the stimulation of PPARα by the pharmacological activator WY14-643 (Figure S5B), and prevented by the PPARα antagonist GW6471 (Figure S5C). The glucagon-stimulated PPARα activation was abolished by the p38 MAPK inhibitor SB203580 (Figure 6D). Furthermore, fasting increases PPARα interaction with p38MAPK in Gcgr+/+ mice, but not in Gcgr−/− mice (Figure 6E), and this increased interaction is mimicked by glucagon (Figure 6F). These findings demonstrate that glucagon activates PPARα in an AMPK- and p38 MAPK-dependent pathway.

We next examined the expression of other transcription factors involved in the regulation of hepatic lipid metabolism. The changes in expression of SREBP1, PGC1a, and ChREBP during fasting were not mimicked by glucagon administration, and/or were not regulated by glucagon or Gcgr genotype in a consistent manner in male and female mice (Figures S5D, S5E, and S5F), whereas male and female mice display similar phenotypes in terms of plasma lipid levels (Figures 1 and S1) and gene expression (Figures 4 and S3) after fasting.

As FGF-21 and Acyl CoA Oxidase (ACO) have been identified as downstream targets of PPARα capable of regulating fasting lipid metabolism (Badman et al., 2007; Inagaki et al., 2007), we assessed ACO and FGF-21 expression in Gcgr−/− mice and in WT mice treated for 24 hr with glucagon. Both mRNA transcripts were induced in Gcgr+/+ liver after fasting (Figures S6A and S6C); however, basal levels of both mRNAs were higher in Gcgr−/− versus Gcgr+/+ mice and did not increase further with fasting (Figures S6A and S6C). Furthermore, glucagon had

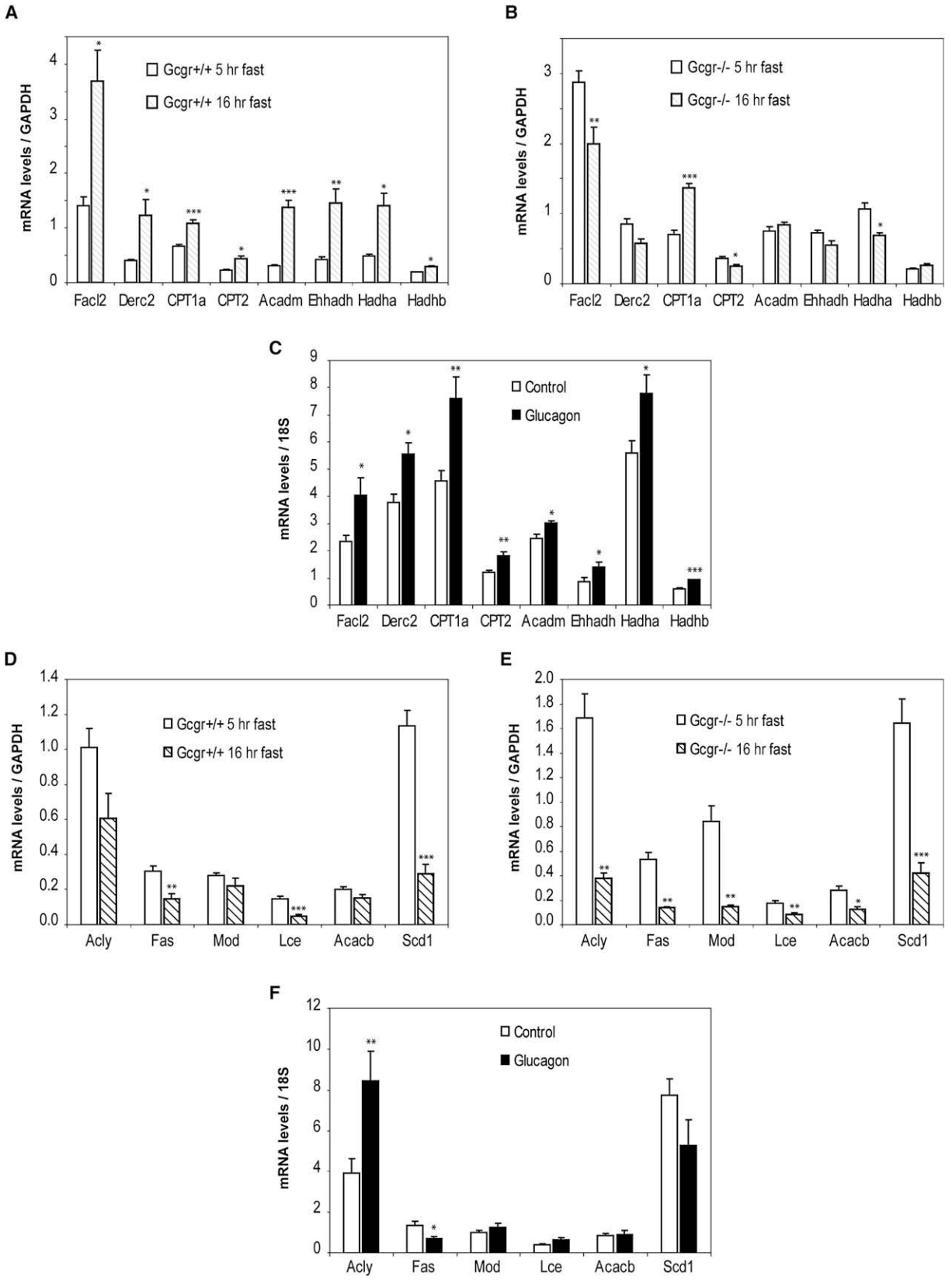
A
mRNA levels / GAPDH
Gcgr+/+ 5 hr fast
Gcgr+/+ 16 hr fast
Facl2 Derc2 CPT1a CPT2 Acadm Ehhadh Hadha Hadhb
B
mRNA levels / GAPDH
Gcgr-/- 5 hr fast
Gcgr-/- 16 hr fast
Facl2 Derc2 CPT1a CPT2 Acadm Ehhadh Hadha Hadhb
C
mRNA levels / 18S
Control
Glucagon
Facl2 Derc2 CPT1a CPT2 Acadm Ehhadh Hadha Hadhb
D
mRNA levels / GAPDH
Gcgr+/+ 5 hr fast
Gcgr+/+ 16 hr fast
Acly Fas Mod Lce Acacb Scd1
E
mRNA levels / GAPDH
Gcgr-/- 5 hr fast
Gcgr-/- 16 hr fast
Acly Fas Mod Lce Acacb Scd1
F
mRNA levels / 18S
Control
Glucagon
Acly Fas Mod Lce Acacb Scd1

no effect on hepatic FGF-21 or ACO expression in WT mice (Figures S6B and S6D). Additionally, circulating levels of FGF-21 were not significantly different after fasting in Gcgr−/− versus Gcgr+/+ mice, and glucagon administration had no effect on levels of circulating FGF-21 in Gcgr+/+ mice (Figures S6E and S6F). Hence, the effects of glucagon on hepatic lipid synthesis and secretion are not associated with corresponding changes in FGF-21 expression.

Glucagon Modulates Triglyceride Synthesis and FFA Beta Oxidation in a PPARα-Dependent Manner

We next investigated the role of PPARα in the modulation of hepatic lipid metabolism by glucagon. No significant difference in FFA neosynthesis was observed in PPARα−/− hepatocytes under basal or glucagon-stimulated conditions (Figure 7A). Although glucagon inhibited TG synthesis in +/+ hepatocytes, glucagon failed to inhibit TG synthesis in PPARα−/− hepatocytes (Figure 7B). In contrast the inhibitory effects of glucagon on TG secretion were preserved in PPARα−/− hepatocytes (Figure 7C, 50.3% inhibition in PPARα+/+ versus 35.2% inhibition in PPARα−/−). Similarly, the hypolipidemic effect of glucagon on levels of plasma FFA and TG as well as the glucagon-mediated inhibition of hepatic triglyceride secretion was preserved in PPARα−/− mice (Figures S7A, S7B, and S7C).

PPARα was also essential for the ability of glucagon to regulate FAO, as glucagon stimulated $^{14}CO_2$ production in PPARα+/+ hepatocytes, but had no effect on FAO in PPARα−/− mice (Figure 7D). Furthermore, in contrast to the glucagon-regulated FAO gene expression profile observed in +/+ mice (Figure 4C), glucagon failed to modulate the expression of multiple genes involved in FFA beta oxidation in PPARα−/− mice (Figure S7D). Finally, pharmacological activation of PPARα in using fenofibrate restored normal levels of FFA beta oxidation in Gcgr−/− liver homogenates (compare Figure 3D versus 6E), increasing FFA beta oxidation by Gcgr−/− liver homogenates to similar levels obtained with Gcgr+/+ liver homogenates. Taken together, these findings indicate that glucagon stimulates TG synthesis and FFA beta oxidation in a PPARα-dependent manner, and is required for the activation of PPARα-dependent metabolic pathways during fasting.

DISCUSSION

Glucagon levels are elevated in subjects with type 2 diabetes and contribute to the development of excess hepatic glucose production and hyperglycaemia. Accordingly, Gcgr antagonists and antisense oligonucleotides (ASOs) directed against the Gcgr are being assessed for the treatment of T2DM; however, the consequences of blocking hepatic Gcgr signaling remain incompletely understood. Our data demonstrate that in the fasted state, glucagon action is essential for multiple pathways regulating lipid homeostasis. Furthermore, the actions of glucagon on lipid metabolism are mediated predominantly through AMPK-, p38 MAPK-, and PPARα-dependent mechanisms.

Analysis of lipid homeostasis in Gcgr−/− mice fasted for 5 hr did not reveal differences in levels of plasma TGs in Gcgr−/− versus Gcgr+/+ littermate controls, consistent with earlier findings (Gelling et al., 2003). In contrast a marked increase in plasma TGs was observed in Gcgr−/− mice after a more prolonged fast. Consistent with the improvement in hyperglycemia, levels of plasma and hepatic TGs were reduced in diabetic rodents following reduction of hepatic Gcgr expression; in contrast, the levels of plasma and liver TGs were paradoxically increased in control nondiabetic rats after ASO administration (Sloop et al., 2004). Similarly, treatment of db/db mice for 3 weeks with Gcgr ASOs resulted in a decrease in liver glycogen but a significant increase in liver TGs in both the fasted and fed state (Liang et al., 2004). Hence, the available evidence suggests that the hepatic TG accumulation observed in fasted Gcgr−/− mice does not simply reflect abnormalities arising due to developmental loss of Gcgr signaling, but rather implicates a relationship linking diminished or absent Gcgr expression with the accumulation of hepatic TG.

FFA beta oxidation/ketogenesis is increased while lipogenesis is decreased during fasting, a state characterized by reduced levels of insulin and increased levels of glucagon and FFA. Studies using PPARα−/− mice have demonstrated the central importance of PPARα signaling pathways for the control of the adaptive metabolic response to fasting (Kersten et al., 1999). Remarkably, Gcgr−/− mice exhibit increased hepatic TG secretion following fasting and enhanced susceptibility to hepatosteatosis following exposure to a high-fat diet (Figure S8), features identical to those previously described in studies of PPARα−/− mice (Kersten et al., 1999). Consistent with the importance of the Gcgr for the adaptive response to fasting, we observed increased expression of genes involved in beta oxidation and an increased capacity of liver to oxidize FFA during the fasted state in Gcgr+/+ mice. However, this gene expression signature was abolished in Gcgr−/− mice, which displayed defective oxidation of FFAs in both the fed and fasted state. Conversely, administration of glucagon further augmented the expression of genes regulating FAO and increased FFA oxidation in WT hepatocytes. Hence, the results of experiments employing either loss or enhanced Gcgr signaling implicate an essential physiological role for Gcgr signaling in the control of a gene expression program linking fasting to enhanced fatty acid oxidation. Furthermore, our data demonstrate that glucagon not only increases the capacity of hepatocytes to oxidize FFA but also increases the availability of substrate for beta oxidation, as

Figure 4. Hepatocyte Gene Expression Profiles following Fasting

(A–E) Real-time PCR was performed on RNA extracted from liver of male Gcgr−/− and littermate control +/+ mice after 5 hr or 16 hr fasting (A, B, D, and E), and from WT males repeatedly injected with glucagon as described in methods (C and F). The relative level of mRNA transcripts detected was normalized to levels of GAPDH (A and B) or 18S (C). All data are mean ± SEM (n = 4–11 mice in each group) and P values are assessed by one-way ANOVA test for comparison of gene expression * = $p < 0.05$; ** = $p < 0.01$; *** = $p < 0.001$ for differences in 5 hr versus 16 hr fasted mice (A, B, D, and E) or for vehicle versus glucagon-treated mice (C and D). Facl2: fatty acid CoA ligase, long chain, 2; Decr2: 2-4-dienoyl-coenzyme A reductase 2, peroxisomal; CPT1a: carnitine palmitoyltransferase 1A; CPT2: carnitine palmitoyltransferase 2; Acadm: acyl-coenzyme A dehydrogenase, medium chain; Ehhadh: enoyl-coenzyme A, hydratase/3-hydroxyacyl coenzyme A dehydrogenase (peroxisomal bifunctional enzyme); Hadha: hydroxyacyl-coenzyme A dehydrogenase/3-ketoacyl-coenzyme A thiolase/enoyl-coenzyme A hydratase (mitochondrial trifunctional protein), alpha subunit; Hadhb: hydroxyacyl-coenzyme A dehydrogenase/3-ketoacyl-coenzyme A thiolase/enoyl-coenzyme A hydratase (mitochondrial trifunctional protein), beta subunit. Acly: ATP citrate lyase; Fas: fatty acid synthase; Mod: malic enzyme; Lce: long chain fatty acid elongase; Acacb: acetyl-coenzyme A carboxylase beta; SCD1: stearoyl-coenzyme A desaturase 1.

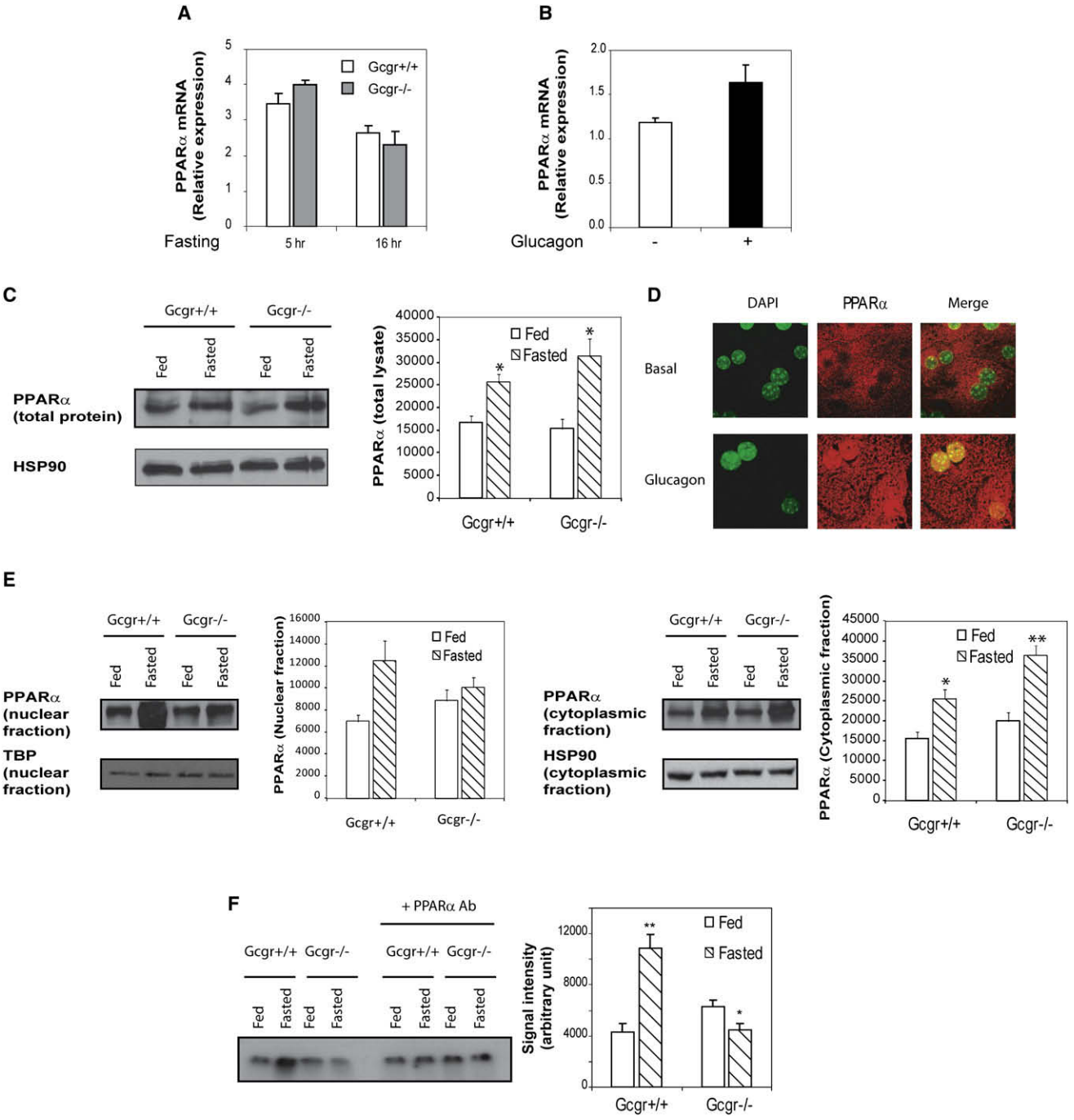

Figure 5. Glucagon Activates PPARα in a p38 MAPK- and AMPK-Dependent Manner

(A and B) Quantification of hepatic PPARα mRNA transcripts from male Gcgr−/− versus Gcgr+/+ littermate controls fasted for 5 or 16 hr (A) or from WT male mice following chronic glucagon administration (B). Data are mean ± SEM (n = 4–11 mice in each group).

(C) Total liver lysates from Gcgr+/+ and Gcgr−/− either fed or fasted for 16 hr were subjected to western blot analysis as described in the Experimental Procedures. * = $p < 0.05$ for levels of proteins in the fed versus fasted state. Data are mean ± SEM (n = 4 mice in each group).

(D) Immunofluorescence staining of PPARα protein in primary mouse hepatocytes cultured in vitro with or without 20 nM glucagon for 30 min.

(E) Nuclear (left panel) and cytoplasmic (right panel) fractions were purified from liver of Gcgr+/+ and Gcgr−/− either fed or fasted for 16 hr, and nuclear proteins were analyzed by western blotting as described in the Experimental Procedures. HSP90 (cytoplasmic fraction) and TATA-binding protein (TBP) (nuclear fraction) were used as loading controls. No HSP90 was detectable in the nuclear fraction, and no TBP was detectable in cytoplasmic fraction (data not shown); * = $p < 0.05$ for levels of proteins in the fed versus fasted state. Data are mean ± SEM (n = 4 mice in each group).

(F) Gel-shift motility assay was performed using nuclear extract from liver of Gcgr−/− mice or littermate controls either fed or fasted for 16 hr, incubated with a radiolabeled ACO probe as described in the Experimental Procedures. Data are mean ± SEM of four independent experiments. * = $p < 0.05$, ** = $p < 0.01$ for fed versus fasted mice.

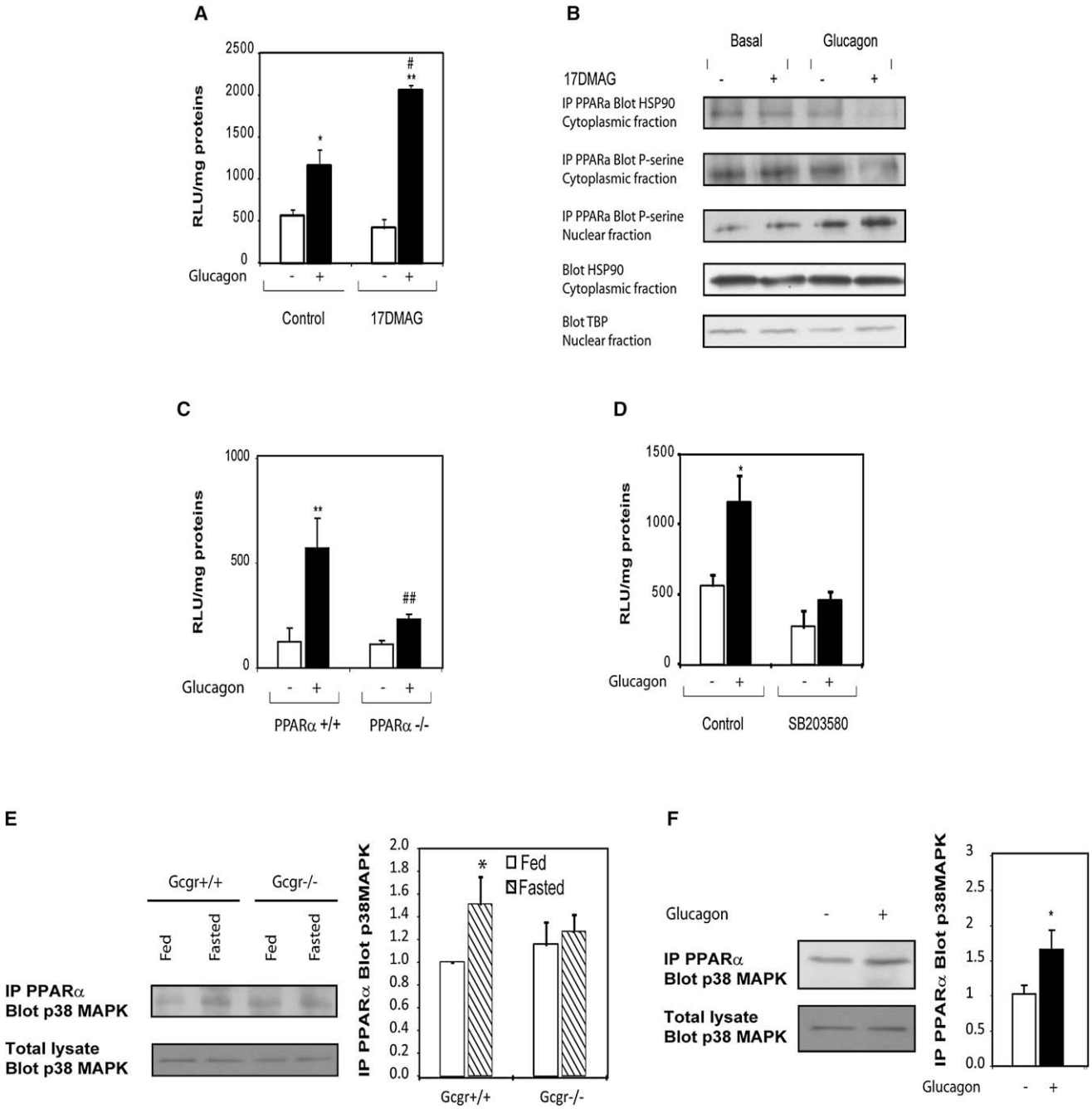

Figure 6. Glucagon Activates PPARα in a p38 MAPK- and AMPK-Dependent Manner

(A–D) Primary hepatocytes prepared from PPARα+/+ or PPARα−/− mice (C) or from WT mice (A and D) were transfected with the PPAR-responsive luciferase reporter pHD(X3)Luc, and further incubated for 24 hr with vehicle alone or 20 nM glucagon, with or without 10 μM SB203580 (D) or with or without 500 nM 17DMAG (A). Data are mean ± SEM of three experiments. ** = $p < 0.01$ for control versus glucagon-treated cells; ## = $p < 0.01$ for glucagon-stimulated PPARα+/+ versus PPARα−/− hepatocytes or glucagon treatment in control versus SB203580-treated hepatocytes. In (B), after 30 min stimulation with 20 nM glucagon with or without 500 nM 17 DMAG, nuclear and cytoplasmic fractions were purified from primary WT hepatocytes. PPARα was immunoprecipitated in each fraction and blotted for HSP90 (upper panel) or phosphoserine (lower panels) HSP90 (cytoplasmic fraction) and TATA-binding protein (TBP) (nuclear fraction) were used as loading controls.

(E and F) PPARα was immunoprecipitated from liver lysate prepared from Gcgr+/+ and Gcgr−/− fed or fasted for 16 hr (E), or from WT mice injected with glucagon (F), then subjected to western blot analysis using an anti-p38 MAPK antibody. Total p38MAPK in total lysate is shown as a loading control.

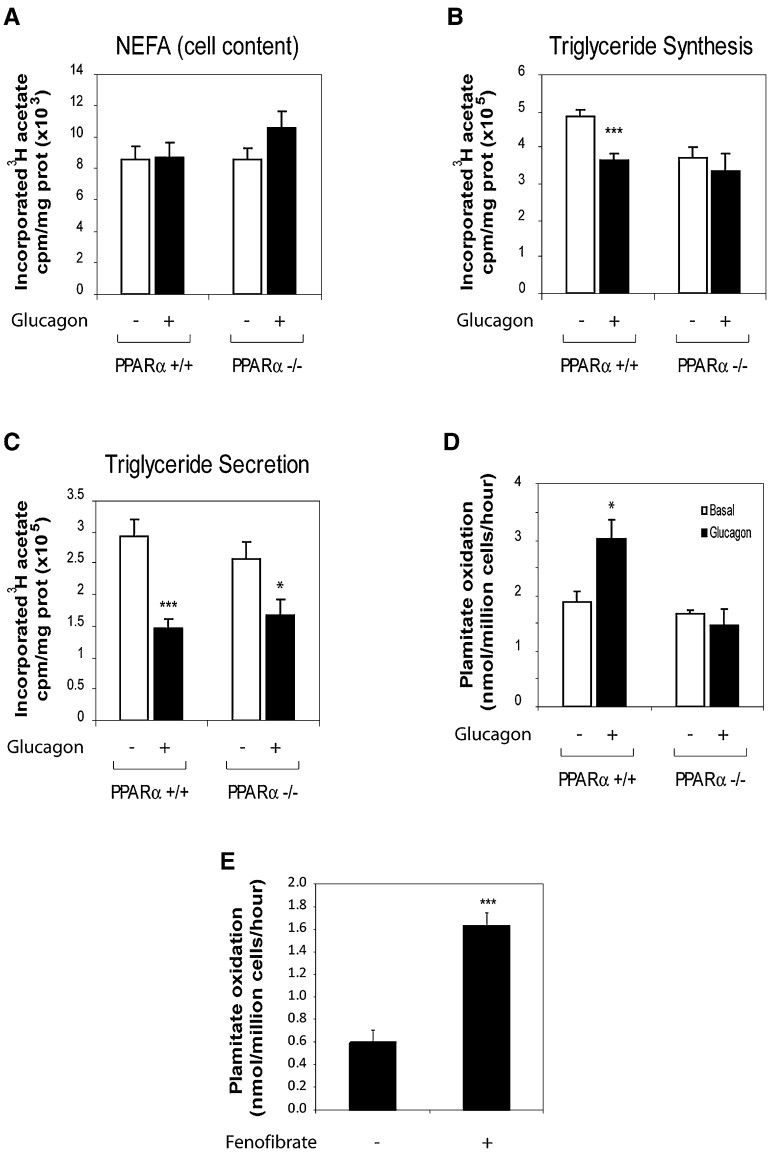

Figure 7. Glucagon Increases FAO and Inhibits TG Synthesis in a PPARα-Dependent Manner

(A–C) Lipid synthesis was assessed by measurement of FFAs and TGs in hepatocytes from WT and PPARα−/− mice treated for 16 hr with or without 20 nM glucagon. Lipids were extracted from the media (secretion) or cells + media (synthesis), separated by TLC, and quantified by scintillation counting. Data are mean ± SEM of four independent experiments. * = $p < 0.05$, *** = $p < .001$ for values obtained in the presence or absence of glucagon.

(D) Beta oxidation of [^{14}C]-palmitate assessed in primary hepatocytes from WT or PPARα−/− mice and treated with or without 20 nM glucagon for 24 hr as described in the Experimental Procedures. Data are mean ± SEM. of four independent experiments. * = $p < 0.05$ for values obtained in the presence or absence of glucagon.

(E) Beta oxidation of [1-^{14}C]-palmitate assessed in liver homogenates prepared from Gcgr−/− fasted for 24 hr with or without fenofibrate administration during fasting as described in the Experimental Procedures. Data are mean ± SEM of six independent experiments. * = $p < 0.05$ for vehicle versus glucagon treated cells in (C).

suggested by the significant increase in FFAs after glucagon stimulation when FFA beta oxidation is inhibited by etomoxir.

Glucagon is known to suppress lipogenesis in part via repression of sterol regulatory element-binding protein-1c (SREBP-1c) expression (Foretz et al., 1999). Moreover, exogenous glucagon stimulates cyclic AMP formation and cAMP response element-binding protein (CREB) activation, leading to control of a lipogenic gene expression program in a PPARγ-dependent manner (Herzig et al., 2003). Recent studies have implicated a role for exogenous glucagon in the control of lipogenesis via a p38 MAPK-dependent manner (Xiong et al., 2007). Inhibition of p38 leads to enhanced TG accumulation in fat-fed mice, together with increased expression of genes promoting hepatic lipogenesis. Conversely, exogenous glucagon reduced levels of SREBP-1c, SREBP-2, FAS, HMG CoA-R, and FPS mRNA transcripts in hepatocytes in a p38-dependent manner (Xiong et al., 2007). Although we also observed that glucagon reduced TG synthesis and fasting decreased expression of mRNA transcripts for lipogenic enzymes in Gcgr+/+ mice, loss of Gcgr signaling had no impact on the fasting-associated reduction in the lipogenic gene expression program. Hence, although glucagon may act pharmacologically to control lipogenesis through SREBP-1c and p38 MAPK, endogenous Gcgr signaling does not appear to be essential for suppression of a lipogenic gene expression program during fasting. Instead, glucagon directs FFA mobilized from TG stores toward beta oxidation rather than reesterification into triglyceride and secretion.

Classic concepts of glucose homeostasis implicate a central role for glucagon in the fasting state to promote enhanced gluconeogenesis and glycogenolysis. Levels of both circulating glucagon and hepatic PPARα mRNA transcripts are increased by fasting and repressed by glucose (Lefebvre et al., 2006). Fasting is also associated with enhanced TG lipolysis, increased levels of FFA, and increased hepatic fatty acid oxidation, thereby enhancing the availability of fuel substrates for use in peripheral tissues. Our current data extend physiological concepts of glucagon action by demonstrating that Gcgr signaling activates a p38MAPK- and PPARα-dependent signaling network to enhance fatty acid oxidation. Moreover, disruption of endogenous Gcgr signaling impairs the control of fatty acid oxidation during fasting. These findings, summarized in Figure S9, taken together with our observations that Gcgr−/− mice rapidly develop hepatosteatosis following high-fat feeding (Figure S8) may have implications for therapeutic strategies designed to attenuate Gcgr signaling for the treatment of type 2 diabetes.

EXPERIMENTAL PROCEDURES

Animals, Treatments and Reagents

Experiments were carried out using 8- to 12-week-old global Gcgr−/− mice and age and sex-matched littermate control mice in the C57BL/6 background

(Gelling et al., 2003) for comparative analyses. Consistent with previous findings, we observed that food intake and body weight was similar in Gcgr−/− and Gcgr+/+ littermate control mice (Gelling et al., 2003). For experiments employing PPARα−/− mice (Jackson Laboratory), age- and sex-matched 129S1/SvImJ mice were used as WT controls (8 to 12 weeks of age) according to Jackson Laboratory recommendation. All mouse strains were maintained on standard rodent chow (unless otherwise indicated) under a normal 12 hr light/12 hr dark cycle. All experiments were conducted according to protocols and guidelines approved by the Toronto General Hospital Animal Care Committee. To minimize the potential influence of circadian rhythms on experimental outcomes, standardized periods of fasting or experimental analyses were utilized. To test the effect of insulin, WT mice fasted for 5 hr were given 0.7 U/kg of human insulin (Novolin GE, Novo Nordisk) by intraperitoneal injection. To test the effect of repeated glucagon administration, mice were injected subcutaneously (sc) with glucagon (30 μg/kg body weight in 500 μl of 10% gelatine) or 10% gelatine alone, involving a total of four injections over a 24 hr period. Mice were euthanized 1 hr after the last injection; blood was obtained via cardiac puncture; and liver samples were collected, snap frozen in liquid nitrogen, and stored at −80°C until further analysis. For acute glucagon injections, mice were fasted for 5 hr, then injected with glucagon (30 μg/kg body weight via sc injection) in 500 μl of 10% gelatin or with vehicle alone (10% gelatin). H89, SB 203580, and AMPKi were from Calbiochem, San Diego, CA and Etomoxir was from Sigma Aldrich, St. Louis, MO.

In Vivo Hepatic TG Secretion

After fasting and/or glucagon administration, mice were injected via the tail vein with Triton WR-1339 (0.5g/kg diluted 15% in PBS pH 7.4). Blood samples (50 μL) were collected prior to IV injection and at 30 min, 1, 2, and 3 hr after injection.

Biochemical Studies

Blood samples were collected by cardiac puncture or tail vein. For plasma preparation, blood samples were supplemented with trasylol, EDTA, and diprotin and centrifuged at 6,000 rpm at 4°C for 5 min. FFA and TGs were measured using colorimetric assays (NEFA Kit and L-Type TG Kit,Wako Chemicals [Richmond, VA]). Insulin levels were determined using a mouse ultrasensitive insulin Elisa (Alpco Diagnostic). Blood glucose levels were measured using a Glucometer (Ascensia; Bayer HealthCare). FGF21 levels were assessed by radioimmunoassay (Phoenix Pharmaceuticals, Inc.).

Real-Time PCR Analysis of Gene Expression

RNA was extracted from liver using Trizol Reagent according to manufacturer instructions (Sigma-Aldrich, St. Louis, MO). Real-time quantitative PCR reactions were carried out using the TaqMan Gene Expression Assay Universal PCR Master Mix (Applied Biosystems; Foster City, CA) and an ABI Prism 7900 Sequence Detection System (Applied Biosystems; Melbourne, Australia). Values for hepatocyte mRNA transcripts were normalized to the levels of GAPDH, as levels of GAPDH mRNA transcripts were not different between Gcgr+/+ and Gcgr−/− mice and did not change following a 5 or 16 hr fast. Relative values for hepatocyte mRNA transcripts after glucagon administration were obtained by normalizing levels of mRNA transcripts to the levels of 18S rRNA in the same RNA samples, as glucagon administration increased levels of GAPDH mRNA transcripts.

Primary Murine Hepatocyte Cultures

Murine hepatocytes were isolated as previously described (Flock et al., 2007), seeded in Primaria plates (BD Biosciences; Mississauga, ON) and allowed to attach for 2 to 4 hr prior to experimental treatments.

Lipid Synthesis and Secretion in Hepatocytes

Cells were labeled with [H3]acetate (5 μCi/ml) in Williams E medium + 5% FBS for 16 hr and lipids were extracted twice with hexane:isopropanol 3:2 (v/v), the organic solvent was evaporated, and lipids were resuspended in hexane and spotted on a TLC plate. Neutral lipids were separated using ether:diethyl ether:glacial acetic acid 90:10:1 (v/v/v). Zones corresponding to the lipid standard were cut, mixed in scintillation cocktail overnight with gentle agitation, and counted on a Packard liquid scintillation counter. After lipid extraction, cells were digested in 1 ml of 50 mM NaOH and used for protein determination.

PPRE-Luciferase Activity

The PPAR-activated firefly luciferase reporter pHD(X3)Luc, obtained from Dr. J. Capone (McMaster University; Toronto, ON, Canada), contains three tandem copies of the PPRE from the rat enoyl-CoA hydratase/3-hydroxyacyl-CoA dehydrogenase gene upstream of a minimal promoter cloned into the plasmid pCPS-luc. (Zhang et al., 1993). After transfection of the reporter plasmid in Williams E media with lipofectamine 2000 at a ratio 1:3 (μL lipofectamine 2000: μg plasmid) for 5 hr, hepatocytes (1 million per well in 6-well plates) were treated with 20 nM glucagon and/or 10 μM SB203580. After 24 hr, cells were washed three times in ice-cold PBS and lysed in 250 μl of harvest buffer (50 mM Tris/MES pH 7.8, 0.1% Tritton X-100, 1 mM DTT). Luciferase activity was determined using 200 μl of cell lysate by adding 5 μl of luciferase cocktail (150 mM Tris/MES 1 M pH 7.8, 150 mM MgOAc, and 40 mM ATP), and luminescence was assessed in a Berthold Tube Luminometer LB-9507. An aliquot of cell lysate was used for total protein determination.

Preparation of Nuclear Extracts and EMSA Assays

Liver tissue (approximately 50 mg) was minced in 500 μl of homogenization buffer (10 mM HEPES pH 7.9, 10 mM KCl, 0.1 mM EDTA pH 7.4, 0.1 mM EGTA, 1 mM DTT, and protease and phospatase inhibitors). Homogenates were dounced 20 times (pestle B) and incubated on ice for 30 min prior to adding 6% of nonidet P40 10%. After an additional 30 min incubation on ice, homogenates were centrifuged for 1 min at 13000 rpm at 4°C. The pellet containing nuclei was resuspended in 100 μl of buffer containing 20 mM HEPES pH 7.9, 400 mM NaCl, 1 mM EDTA pH 7.4, 1 mM EGTA, 1 mM DTT, and 5% glycerol, supplemented with protease and phosphatase inhibitors. Nuclei were incubated for 30 min on ice, and homogenates were vortexed every 10 min for 10 s. After a final 1 min centrifugation at 13,000 rpm at 4°C, protein concentration determination in supernatant was performed as described previously (Rodriguez et al., 2000).

Immunohistochemistry

Primary hepatocytes were seeded in fibronectin-coated glass slide chambers. After 24 hr culture in Williams E media without serum but supplemented with 2 mM Glutamax, 100 U/ml penicillin, and 100 μg/mL streptomycin, cells were stimulated with 20 nM glucagon for 30 min, after which cells were fixed for 1 hr at room temperature in 4% formaldehyde. After 1 hr blocking in PBST + 10% donkey serum, cells were incubated overnight in a humidified chamber with anti-PPARα antibody (Santa Cruz Biotechnology; Santa Cruz, CA) diluted 1/100 in PBS:1% Triton + 5% bovine serum albumin (BSA). Cells were then incubated for 1 hr at room temperature with Cy2-conjugated donkey anti-rabbit IgG, stained with 4′,6-diamidino-2-phenylindole (DAPI) (1:50,000 in PBS for 15 min), and mounted using Dako fluorescent mounting medium (DakoCytomation Canada; Ontario, Canada). Cells were visualized using an Olympus FluoView FV1000 microscope and a 63X oil immersion objective, using sequential capture.

Western Blot Analysis

Primary mouse hepatocytes were serum-starved for 24 hr in Williams E media supplemented with 2 mM GlutaMAX, 100 U/ml penicillin, and 100 μg/mL streptomycin, then stimulated with 20 nM glucagon in the presence or absence of signal transduction inhibitors added 30 min prior to glucagon. The experiment was terminated by transferring the plates onto ice and washing the cells with ice-cold PBS, and protein samples were prepared as described (Koehler and Drucker, 2006). Antibodies against PPARα (Fitzgerald Industries Intl.; Concord, MA), phospho-p38 MAPK (Thr180/Tyr182), phospho-AMPKα (Thr172), total p38 MAPK, and total AMPK (Cell Signaling Technology; Beverly, MA) were used according to the manufacturer's instructions. Densitometry was performed on blots exposed on Biomax MR films (Eastman Kodak Co.) using a Hewlett-Packard ScanJet 3p scanner and NIH Image software.

p38 MAPK Activity and Protein Analyses

Cells were lysed in 20 μl of lysis buffer, and p38 MAPK assay was performed on 10 μl of lysate using the TruLight p38α Kinase Assay Kit (Calbiochem, La Jolla, CA), according to manufacturer instructions. Cell protein content was measured using BCA kit (Pierce; Rockford, IL), with BSA as the standard.

shRNA-Mediated Knockdown of p38MAPK and AMPK

shRNA plasmid and Trans-lentiviral packaging system were purchased from Open Biosystem (Huntsville, AL). Lentivirus production and hepatocytes

infection were performed according to manufacturer instructions. Lipid synthesis and FFA beta oxidation assays were done 36 hr after infection, as described above and below.

FFA Beta Oxidation in Hepatocytes

FFA oxidation was assessed by measuring the production of $^{14}CO_2$ from [1-^{14}C]palmitate. Briefly, hepatocytes (1 million in a 6 cm plate) were incubated for 24 hr in serum-free Williams E medium containing 20 nM glucagon with or without signal transduction inhibitors. Plates were then washed with warm PBS and 2 ml of beta oxidation media (1 mM palmitate bound to fatty acid-free albumin at a molar ration 5:1 in Williams E medium, 0.3 μCi/mL 1-^{14}C palmitate (Amersham Biosciences; Piscataway, NJ) with or without glucagon and/or inhibitors was added. Each petri dish was sealed with parafilm onto the inside of which a Whatman paper wet with 100 μl of phenylethylamine/methanol (1:1) was taped to trap the CO_2 produced during the incubation period. After a 2 hr incubation period, 200 μl of H_2SO_4 (4 mol/l) was added to the cells, which were then further incubated for 1 hr at 37°C. Finally, the seal was removed from each petri dish, and the pieces of Whatman paper were transferred to scintillation vials for determination of radioactivity. An aliquot of media was counted to determine the total radioactivity.

FFA Beta Oxidation in Liver Homogenates

Half a gram of liver was manually homogenized using a Potter-Elvejhem homogenizer in 10 ml of ice-cold isolation buffer (220 mM mannitol, 70 mM sucrose, 2 mM HEPES, and 0.1 mM EDTA at pH 7.4). Aliquots of homogenate (300 μl) were added to 1.7 ml of reaction medium (50 mM sucrose, 150 mM Tris-HCl, 20 mM KH_2PO_4, 10 mM $MgCl_2$-$6H_2O$, 2 mM EDTA, 1 mM L-carnitine, 0.2 mM CoA, 2 mM NAD, 0.1 mM malate, 10 mM ATP, 1 mM Palmitate complexed to fatty acid-free albumin at a 5:1 molar ratio in Williams E medium, 0.3 μCi of [1-^{14}C]-palmitate [Amersham Biosciences], pH 7.4). Reactions performed in a sealed flask were allowed to proceed for 30 min in a shaking water bath at 37°C. Incubations were terminated by the addition of 1 ml of 3 M perchloric acid to the reaction medium to precipitate protein and nonmetabolized palmitate and then further incubated at room temperature for 2 hr for collection of $^{14}CO_2$ into a suspended well containing 500 μl of ethanolamine. Blanks were prepared by acidification of the reaction medium immediately after the addition of the homogenate. Radioactivity in CO_2 was quantified by liquid scintillation spectrometry.

Statistical Analysis

Statistical significance was assessed by one-way or two-way ANOVA using Bonferroni's multiple comparison posttest and, where appropriate, by unpaired Student's t test using GraphPad Prism 4 (GraphPad Software; San Diego, CA). A p value < 0.05 was considered to be statistically significant.

SUPPLEMENTAL DATA

Supplemental Data include nine figures and can be found online at http://www.cell.com/cellmetabolism/supplemental/S1550-4131(08)00292-1.

ACKNOWLEDGMENTS

C.L. was supported in part by a Research Fellowship Award from the Banting and Best Diabetes Centre, and A.M. was supported in part by a Graduate Studentship Award from the Canadian Diabetes Association. The research was supported by an operating grant from the Canadian Institutes for Health Research MOP-10903 (D.J.D.), by NIH grant RO1 DK47425 to M.C., and the Canada Research Chairs Program (D.J.D.). We thank Marc Angeli for helpful technical advice.

Received: October 13, 2007
Revised: June 3, 2008
Accepted: September 12, 2008
Published: November 4, 2008

REFERENCES

Aromataris, E.C., Roberts, M.L., Barritt, G.J., and Rychkov, G.Y. (2006). Glucagon activates Ca2+ and Cl- channels in rat hepatocytes. J. Physiol. *573*, 611–625.

Badman, M.K., Pissios, P., Kennedy, A.R., Koukos, G., Flier, J.S., and Maratos-Flier, E. (2007). Hepatic fibroblast growth factor 21 is regulated by PPARalpha and is a key mediator of hepatic lipid metabolism in ketotic states. Cell Metab. *5*, 426–437.

Bobe, G., Ametaj, B.N., Young, J.W., and Beitz, D.C. (2003a). Effects of exogenous glucagon on lipids in lipoproteins and liver of lactating dairy cows. J. Dairy Sci. *86*, 2895–2903.

Bobe, G., Ametaj, B.N., Young, J.W., and Beitz, D.C. (2003b). Potential treatment of fatty liver with 14-day subcutaneous injections of glucagon. J. Dairy Sci. *86*, 3138–3147.

Bobe, G., Ametaj, B.N., Young, J.W., Anderson, L.L., and Beitz, D.C. (2006). Exogenous glucagon effects on health and reproductive performance of lactating dairy cows with mild fatty liver. Anim. Reprod. Sci. *102*, 194–207.

Cao, W., Collins, Q.F., Becker, T.C., Robidoux, J., Lupo, E.G., Jr., Xiong, Y., Daniel, K.W., Floering, L., and Collins, S. (2005). p38 Mitogen-activated protein kinase plays a stimulatory role in hepatic gluconeogenesis. J. Biol. Chem. *280*, 42731–42737.

Charbonneau, A., Couturier, K., Gauthier, M.S., and Lavoie, J.M. (2005a). Evidence of hepatic glucagon resistance associated with hepatic steatosis: reversal effect of training. Int. J. Sports Med. *26*, 432–441.

Charbonneau, A., Melancon, A., Lavoie, C., and Lavoie, J.M. (2005b). Alterations in hepatic glucagon receptor density and in Gsalpha and Gialpha2 protein content with diet-induced hepatic steatosis: effects of acute exercise. Am. J. Physiol. Endocrinol. Metab. *289*, E8–E14.

Chen, J., Ishac, E.J., Dent, P., Kunos, G., and Gao, B. (1998). Effects of ethanol on mitogen-activated protein kinase and stress-activated protein kinase cascades in normal and regenerating liver. Biochem. J. *334*, 669–676.

Conarello, S.L., Jiang, G., Mu, J., Li, Z., Woods, J., Zycband, E., Ronan, J., Liu, F., Roy, R.S., Zhu, L., et al. (2007). Glucagon receptor knockout mice are resistant to diet-induced obesity and streptozotocin-mediated beta cell loss and hyperglycaemia. Diabetologia *50*, 142–150.

Eaton, R.P. (1973). Hypolipemic action of glucagon in experimental endogenous lipemia in the rat. J. Lipid Res. *14*, 312–318.

Flock, G., Baggio, L.L., Longuet, C., and Drucker, D.J. (2007). Incretin receptors for glucagon-like peptide 1 and glucose-dependent insulinotropic polypeptide are essential for the sustained metabolic actions of vildagliptin in mice. Diabetes *56*, 3006–3013.

Foretz, M., Pacot, C., Dugail, I., Lemarchand, P., Guichard, C., Le Liepvre, X., Berthelier-Lubrano, C., Spiegelman, B., Kim, J.B., Ferre, P., and Foufelle, F. (1999). ADD1/SREBP-1c is required in the activation of hepatic lipogenic gene expression by glucose. Mol. Cell. Biol. *19*, 3760–3768.

Gelling, R.W., Du, X.Q., Dichmann, D.S., Romer, J., Huang, H., Cui, L., Obici, S., Tang, B., Holst, J.J., Fledelius, C., et al. (2003). Lower blood glucose, hyperglucagonemia, and pancreatic {alpha} cell hyperplasia in glucagon receptor knockout mice. Proc. Natl. Acad. Sci. USA *100*, 1438–1443.

Giordano, A., Calvani, M., Petillo, O., Grippo, P., Tuccillo, F., Melone, M.A., Bonelli, P., Calarco, A., and Peluso, G. (2005). tBid induces alterations of mitochondrial fatty acid oxidation flux by malonyl-CoA-independent inhibition of carnitine palmitoyltransferase-1. Cell Death Differ. *12*, 603–613.

Guettet, C., Mathe, D., Riottot, M., and Lutton, C. (1988). Effects of chronic glucagon administration on cholesterol and bile acid metabolism. Biochim. Biophys. Acta *963*, 215–223.

Guettet, C., Mathe, D., Navarro, N., and Lecuyer, B. (1989). Effects of chronic glucagon administration on rat lipoprotein composition. Biochim. Biophys. Acta *1005*, 233–238.

Guettet, C., Rostaqui, N., Mathe, D., Lecuyer, B., Navarro, N., and Jacotot, B. (1991). Effect of chronic glucagon administration on lipoprotein composition in normally fed, fasted and cholesterol-fed rats. Lipids *26*, 451–458.

Herzig, S., Hedrick, S., Morantte, I., Koo, S.H., Galimi, F., and Montminy, M. (2003). CREB controls hepatic lipid metabolism through nuclear hormone receptor PPAR-gamma. Nature *426*, 190–193.

Hiyoshi, H., Yanagimachi, M., Ito, M., Yasuda, N., Okada, T., Ikuta, H., Shinmyo, D., Tanaka, K., Kurusu, N., Yoshida, I., et al. (2003). Squalene synthase

inhibitors suppress triglyceride biosynthesis through the farnesol pathway in rat hepatocytes. J. Lipid Res. *44*, 128–135.

Inagaki, T., Dutchak, P., Zhao, G., Ding, X., Gautron, L., Parameswara, V., Li, Y., Goetz, R., Mohammadi, M., Esser, V., Elmquist, J.K., Gerard, R.D., Burgess, S.C., Hammer, R.E., Mangelsdorf, D.J., Kliewer, S.A., et al. (2007). Endocrine regulation of the fasting response by PPARalpha-mediated induction of fibroblast growth factor 21. Cell Metab. *5*, 415–425.

Jelinek, L.J., Lok, S., Rosenberg, G.B., Smith, R.A., Grant, F.J., Biggs, S., Bensch, P.A., Kuijper, J.L., Sheppard, P.O., Sprecher, C.A., et al. (1993). Expression cloning and signaling properties of the rat glucagon receptor. Science *259*, 1614–1616.

Jiang, G., and Zhang, B.B. (2003). Glucagon and regulation of glucose metabolism. Am. J. Physiol. Endocrinol. Metab. *284*, E671–E678.

Johnson, D.G., Goebel, C.U., Hruby, V.J., Bregman, M.D., and Trivedi, D. (1982). Hyperglycemia of diabetic rats decreased by a glucagon receptor antagonist. Science *215*, 1115–1116.

Kersten, S., Seydoux, J., Peters, J.M., Gonzalez, F.J., Desvergne, B., and Wahli, W. (1999). Peroxisome proliferator-activated receptor alpha mediates the adaptive response to fasting. J. Clin. Invest. *103*, 1489–1498.

Kimball, S.R., Siegfried, B.A., and Jefferson, L.S. (2004). Glucagon represses signaling through the mammalian target of rapamycin in rat liver by activating AMP-activated protein kinase. J. Biol. Chem. *279*, 54103–54109.

Koehler, J.A., and Drucker, D.J. (2006). Activation of GLP-1 receptor signaling does not modify the growth or apoptosis of human pancreatic cancer cells. Diabetes *55*, 1369–1379.

Koo, S.H., Flechner, L., Qi, L., Zhang, X., Screaton, R.A., Jeffries, S., Hedrick, S., Xu, W., Boussouar, F., Brindle, P., et al. (2005). The CREB coactivator TORC2 is a key regulator of fasting glucose metabolism. Nature *437*, 1109–1111.

Lefebvre, P., Chinetti, G., Fruchart, J.C., and Staels, B. (2006). Sorting out the roles of PPAR alpha in energy metabolism and vascular homeostasis. J. Clin. Invest. *116*, 571–580.

Liang, Y., Osborne, M.C., Monia, B.P., Bhanot, S., Gaarde, W.A., Reed, C., She, P., Jetton, T.L., and Demarest, K.T. (2004). Reduction in Glucagon Receptor Expression by an Antisense Oligonucleotide Ameliorates Diabetic Syndrome in db/db Mice. Diabetes *53*, 410–417.

Mayo, K.E., Miller, L.J., Bataille, D., Dalle, S., Goke, B., Thorens, B., and Drucker, D.J. (2003). International Union of Pharmacology. XXXV. The Glucagon Receptor Family. Pharmacol. Rev. *55*, 167–194.

Nafikov, R.A., Ametaj, B.N., Bobe, G., Koehler, K.J., Young, J.W., and Beitz, D.C. (2006). Prevention of fatty liver in transition dairy cows by subcutaneous injections of glucagon. J. Dairy Sci. *89*, 1533–1545.

Otway, S., and Robinson, D.S. (1967). The use of a non-ionic detergent (Triton WR 1339) to determine rates of triglyceride entry into the circulation of the rat under different physiological conditions. J. Physiol. *190*, 321–332.

Patsouris, D., Reddy, J.K., Müller, M., and Kersten, S. (2006). Peroxisome proliferator-activated receptor alpha mediates the effects of high-fat diet on hepatic gene expression. Endocrinology *147*, 1508–1516.

Prip-Buus, C., Pegorier, J.P., Duee, P.H., Kohl, C., and Girard, J. (1990). Evidence that the sensitivity of carnitine palmitoyltransferase I to inhibition by malonyl-CoA is an important site of regulation of hepatic fatty acid oxidation in the fetal and newborn rabbit. Perinatal development and effects of pancreatic hormones in cultured rabbit hepatocytes. Biochem. J. *269*, 409–415.

Raskin, P., and Unger, R.H. (1978). Hyperglucagonemia and its suppression. Importance in the metabolic control of diabetes. N. Engl. J. Med. *299*, 433–436.

Rodriguez, C., Noe, V., Cabrero, A., Ciudad, C.J., and Laguna, J.C. (2000). Differences in the formation of PPARalpha-RXR/acoPPRE complexes between responsive and nonresponsive species upon fibrate administration. Mol. Pharmacol. *58*, 185–193.

Scanu, A.M. (1965). Factors affecting lipoprotein metabolism. Adv. Lipid Res. *3*, 63–138.

Sloop, K.W., Cao, J.X., Siesky, A.M., Zhang, H.Y., Bodenmiller, D.M., Cox, A.L., Jacobs, S.J., Moyers, J.S., Owens, R.A., Showalter, A.D., et al. (2004). Hepatic and glucagon-like peptide-1-mediated reversal of diabetes by glucagon receptor antisense oligonucleotide inhibitors. J. Clin. Invest. *113*, 1571–1581.

Sumanasekera, W.K., Tien, E.S., Davis, J.W., 2nd, Turpey, R., Perdew, G.H., and Vanden Heuvel, J.P. (2003a). Heat shock protein-90 (Hsp90) acts as a repressor of peroxisome proliferator-activated receptor-alpha (PPARalpha) and PPARbeta activity. Biochemistry *42*, 10726–10735.

Sumanasekera, W.K., Tien, E.S., Turpey, R., Vanden Heuvel, J.P., and Perdew, G.H. (2003b). Evidence that peroxisome proliferator-activated receptor alpha is complexed with the 90-kDa heat shock protein and the hepatitis virus B X-associated protein 2. J. Biol. Chem. *278*, 4467–4473.

Unger, R.H. (1971). Glucagon physiology and pathophysiology. N. Engl. J. Med. *285*, 443–449.

Unson, C.G., Gurzenda, E.M., and Merrifield, R.B. (1989). Biological activities of des-His1[Glu9]glucagon amide, a glucagon antagonist. Peptides *10*, 1171–1177.

Wakelam, M.J., Murphy, G.J., Hruby, V.J., and Houslay, M.D. (1986). Activation of two signal-transduction systems in hepatocytes by glucagon. Nature *323*, 68–71.

Xiong, Y., Collins, Q.F., Jie, A., Lupo, E., Jr., Liu, H.Y., Liu, D., Robidoux, J., Liu, Z., and Cao, W. (2007). p38 mitogen-activated protein kinase plays an inhibitory role in hepatic lipogenesis. J. Biol. Chem. *282*, 4975–4982.

Zhang, B., Marcus, S.L., Miyata, K.S., Subramani, S., Capone, J.P., and Rachubinski, R.A. (1993). Characterization of protein-DNA interactions within the peroxisome proliferator-responsive element of the rat hydratase-dehydrogenase gene. J. Biol. Chem. *268*, 12939–12945.